Hindawi
International Journal of Polymer Science
Volume 2022, Article ID 9649726, 10 pages
https://doi.org/10.1155/2022/9649726

Research Article

Development and Characterization of Pullulan-Carboxymethyl Cellulose Blend Film for Packaging Applications

Murugesan Thangavelu and Senthil Vadivu Kulandhaivelu

Department of Printing Technology, College of Engineering Guindy, Anna University, Chennai, 600025 Tamil Nadu, India

Correspondence should be addressed to Murugesan Thangavelu; muruksun@gmail.com

Received 1 April 2022; Revised 31 May 2022; Accepted 1 June 2022; Published 16 June 2022

Academic Editor: Debora Puglia

Edible packaging materials have widespread applications in pharmaceutical industries. In this study, the physical, thermal, colour, mechanical, and water barrier properties of a novel edible film based on pullulan (PUL) and carboxymethyl cellulose (CMC) were investigated. The blend films were made by the solution casting method with 3 g of total solid content. The following percentages of 100/0, 75/25, 50/50, 25/75, and 0/100 were used to prepare the films. Fourier transform infrared (FTIR) spectroscopy, X-ray diffraction (XRD), scanning electron microscopy (SEM), and thermogravimetric analysis (TGA) were used to analyze the interaction between PUL and CMC. At the level of 75/25 percentage of PUL, CMC film showed the lowest EAB% (5.55%), the highest values for TS (17.30 MPa), WVP value (4.12×10^{-10} g m^{-1}s^{-1}Pa^{-1}), and water contact angle of 63.43°. By increasing the CMC concentration, blend films became slightly greenish and yellowish but appeared transparent with UV blocking ability. This study reveals that 75/25 (PUL/CMC) blend film has a good potential that can be used in producing edible packaging films to protect the quality of pharmaceutical products with interesting specifications.

1. Introduction

Packaging materials play an essential role in protecting products from the outside environment, and this holds true for food, biomedical, and industrial packaging [1]. In the market, thermoplastics are used to protect and preserve products. Plastics used in current commerce exceed 5 trillion tons, with an annual growth rate of about 5%, indicating the biggest area of application for crude oil. It emphasizes how oil-dependent the nondegradable plastic business is and how rising crude oil prices may have a financial effect on the plastic trade. As a result, biopolymer materials have been used as an alternative raw material because of their environmental friendliness, degradability, and sustainability [1, 2]. Edible films based on starch are extensively used as an edible and food preservation medium [3]. Many research studies have been conducted to explore the characteristics of starch-based edible films [4–8]. However, starch-based films' development is hampered by weak physical characteristics and high susceptibility to moisture [9]. Many researchers used polysaccharides and protein to enhance edible films' strength [10–12]. Polysaccharides are a kind of carbohydrate that comes in a variety of forms, and their derivatives are applied to make edible films. Polysaccharide blend films may be used to minimize gas migration inside the pack and add beneficial substances to food to enhance its characteristics [13].

PUL is a macromolecule biopolymer made from Aureobasidium pullulans, which is found in sugar culture and starch. It has a simple molecular structure and a linear chain obtained by polymerization through the α-(1→6) glycoside and α-(1→4) glycoside linkages, as reported by Shao et al. [14]. As a result of the unique linking arrangement, PUL film has different physical characteristics. Furthermore, the generated film has a good film-forming capacity and is odorless, tasteless, clear, heat sealable, and soluble in cold and hot water. It has excellent oxygen barrier characteristics and inhibits fungal development in packed products [15, 16]. Pullulan is a polysaccharide that may be combined with other polysaccharides to make a food preservative, film, or coating material [17, 18]. Another major polysaccharide-CMC is used to replace nonbiodegradable packaging

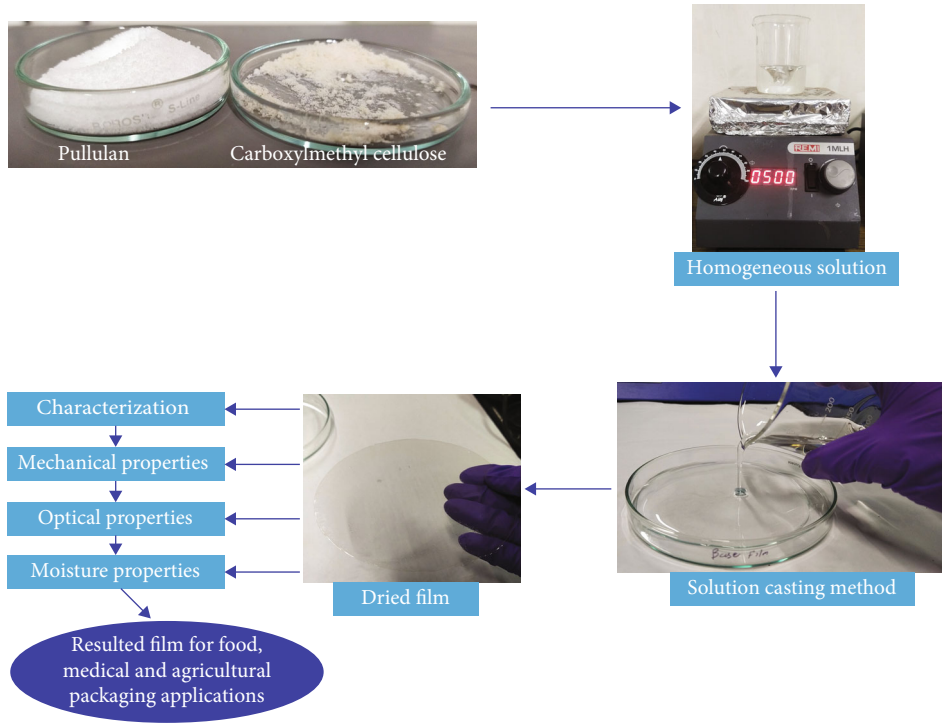

Figure 1: Graphical explanation of edible film fabrication process of PUL-CMC.

material in the market. Its chemical formula is C8H15NaO8, and it has a strong hydrogen bond that adds to the materials' strength. The semisynthetic derivative of fiber cellulose is made by substituting carboxymethyl groups for 2, 3, and 6 hydroxyl groups of fiber cellulose [19]. As a cellulose derivative, beta-(1,4)-D-glucopyranose polymer exhibits excellent film formation, moisture, oil, and oxygen barrier characteristics [20]. Several studies on the material characteristics of PUL with various polysaccharides and starch materials have been published [2, 21, 22]. Similarly, CMC with various polysaccharides has been reported [16, 20].

There is a paucity of data on edible films made by PUL and CMC. To take advantage of the novel pullulans' cost-effectiveness, it is combined with CMC to prepare edible films for packaging application. As a result, it is important to define their blends to ensure that the materials' characteristics stay acceptable. PUL and CMC were mixed in various percentages, to produce the edible film. The physical, UV barrier, mechanical, optical, and water-related characteristics of the resultant films were studied. The current research covers the development and characterization of novel edible film for pharmaceutical packaging applications.

2. Materials and Methods

2.1. Materials. Pullulan TCI-P0978 was acquired from Tokyo Chemical Industry Co., Ltd. (Tokyo, Japan). The molecular weight (M_w) of PUL = 1.5×10^4 g mol^{-1}. The carboxymethyl cellulose CMC was obtained from Sigma-Aldrich Chemicals Private Limited, Bangalore, India, and the molecular weight (M_w) is 2.621×10^5 g mol^{-1}. Glycerol (Gly) was procured from Merck Life Science Private Limited, Mumbai, India. The molecular weight (M_w) of Gly = 92.1 g/mol^{-1}, and all other chemical reagents were of analytical grade.

2.2. Preparation of Film-Forming Solution. The film-forming solutions were produced by *w*/*v* and mixed with percentages of 100/0, 75/25, 50/50, 25/75, and 0/100, as reported by Lupina et al. [23]. Samples were coded as S1, S2, S3, S4, and S5, and the total solid content was 3 g. To complete gelatinization, glycerol 30% (*w*/*v*) was added to film-making solutions, and the film was produced using the solution casting technique Figure 1. Separately, PUL was processed in 50 mL cold distilled water at room temperature for 2 hours at 350 RPM on a universal hot plate magnetic stirrer, and CMC was dissolved in 50 mL distilled water at 50°C for 3 hours at 550 RPM. Afterward, both were combined and stirred for an hour to create a film-making solution. The gelatinized solution was maintained at a constant temperature of 2°C until all air bubbles had vanished. The prepared solutions were poured onto a 15 cm × 1.5 cm Petri dish according to the above percentage and dried for 72 hours at 40°C to create a flawless film. After the films were completely dried, they were put in a climatic chamber at 25°C and 65% relative humidity (RH) for 24 hours. Further, the peeled films were stored in a desiccator.

2.3. Fourier Transform Infrared (FTIR) Spectrometry. The molecular structure of the blend films was investigated using FTIR spectroscopy (Shimadzu Corporation, Kyoto, Japan). The measurements were made at 20°C in a dry atmosphere with 45 scans per sample and a resolution of 8 cm^{-1}.

2.4. XRD Analysis. The structural order of the produced films was determined using an X-ray diffractometer (X-Pert Pro PANalytical, UK) with copper k-α radiation source ($\lambda = 0.15406$ nm), 30 kV, 10 mA, static dispersion slit, diverging slit size of 0.4354°, and 0.1-inch receiver slit. The step size was 0.01° and the count duration was 5.7 seconds per step in the two bands, and the film samples were scanned in the 2θ range of 10-80°.

2.5. Scanning Electron Microscopy (SEM). SEM images of the surface from obtained films were acquired using a VEGA III SBU (TESCAN) scanning electron microscope operating in the high vacuum/secondary electron module of the system at an accelerating voltage of 5-20 kV. The samples were placed on a bronze substrate, and a vacuum was applied before being sputter-coated with a thin coating of gold. It was tilted to 30°, for observation at a magnification of 5000x.

2.6. Thermogravimetric Analysis (TGA). Thermogravimetric analysis was used to determine the weight loss tendency and heat resistance of all the produced films by using Seiko EXSTAR 6000 TGA/DTA instrument. The produced films were burned at a rate of 20°C/min from 28°C to 1000°C in a nitrogen environment.

2.7. Thickness and Density Measurement. The thickness of the produced film samples was measured using a digital micrometer (MDC-25SB, Mitutoyo Corporation, Kanagawa, Japan) with an accuracy of 0.001 mm at five locations in each sample. The mean thickness was calculated for each sample, and the following formula was used to determine the density of the film [24]:

$$\rho = \frac{m}{S \times d}, \tag{1}$$

where ρ is density (g/cm^3), m is film mass, S is the film area, and d is film thickness.

2.8. Mechanical Properties. The films' tensile strength and elongation were measured using a Universal Testing Machine (UTM, H10KS, Tinius Olsen, UK) with minor modifications to ASTM D882 [25]. The films were sliced into 12 cm × 2.5 cm rectangular pieces and fastened into the grips. The initial grip separation was maintained at 10 cm length and 5 cm/min crosshead speed. Tensile strength and elongation are expressed in MPa and percentage, accordingly. Formulae (2) and (3) were used to determine tensile strength and elongation. Each report's results corresponded to at least three different measurements.

$$\text{Tensile strength (MPa)} = \frac{\text{Force } (N)}{\text{Thickness (mm)} \times \text{Width (mm)}}, \tag{2}$$

$$\text{Elongation (\%)} = \frac{L_i - L_0}{L_i} \times 100, \tag{3}$$

where L_0 is the initial length of the film and L_i is the length of film at the break.

2.9. Colour Parameters. The colour characteristics of the blend films were determined using a spectrophotometer SS5100H (Premier Colorscan Instruments Pvt. Ltd., Navi Mumbai, India). To prevent any light trapping, the viewable region was made much bigger than the lighted area. The colour measurements of the films were carried out against a white standard colour plate ($L = 97.75$, $a = 0.49$, $b = 1.96$) that had been used for the calibration of the equipment. It was necessary to use the following colour parameters: $L*$ (100: white and 0: black), $a*$ (+60: red and -60: green), and $b*$ (+60: yellow and -60: blue). The C illuminant and the 2° observer were used to conduct the experiments. To compute yellowness index (YI), whiteness index (WI), and the colour difference ΔE, formulae (4), (5), and (6) were used in conjunction with the usual test procedure.

$$\text{YI} = \frac{142.86b}{L}, \tag{4}$$

$$\text{WI} = 100 - \sqrt{(100 - \text{L})^2 + a^2 + b^2}, \tag{5}$$

$$\Delta E = \sqrt{(L^* - L)^2 + (a^* - a)^2 + (b^* - b)^2}. \tag{6}$$

2.10. Light Barrier Properties. The transmittance capacity of ultraviolet and visible light was evaluated using a UV-Vis spectrophotometer (model UH5300, UV-Vis spectrophotometer, Hitachi-High Tech Science Corporation, Tokyo, Japan). This analysis is intended for the packaging of drugs in capsules, which may lose their newness and desirability when exposed to UV and visible light. Ultraviolet and visible light barrier characteristics of produced films were tested from 200 nm to 800 nm. The samples were sliced into 2 cm × 3 cm pieces and put within the spectrophotometer holder. Measurements were collected from three pieces in each of the three samples, and the average transparency was calculated using

$$\%T = \frac{T_f}{T_B} \times 100, \tag{7}$$

where T_f represents the intensity of lightweight specimen in the beam and T_B represents the light intensity without the sample in the beam [26].

2.11. Moisture Content. The moisture content of film samples (2 cm × 2 cm) was examined gravimetrically by the oven drying method at 103 ± 2°C for 24 hours. The moisture content was calculated using the following formula:

$$MC = \frac{W_i - W_f}{W_i} \times 100, \tag{8}$$

where W_i is the weight of initial film and W_f is the weight of dried film [19].

2.12. Contact Angle. A contact angle meter was used to evaluate the surface wettability of the samples (Holmarc, India). The film was placed on the sample base, and a drop of 10 μL

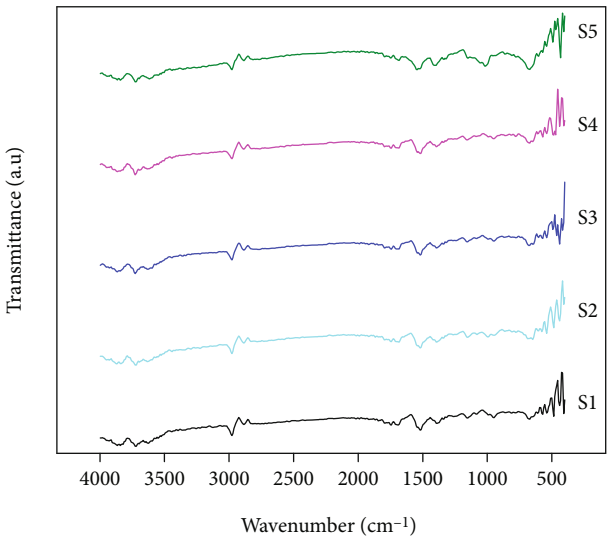

Figure 2: FTIR spectrum of PUL-CMC blend films (S1-100/0, S2-75/25, S3-50/50, S4-25/75, and S5-0/100).

water was applied to the film's surface using a microsyringe. The contact angle (θ) of both sides of the water droplet was measured at room temperature. To get the average value, the experiment was performed 5 times for each film sample.

2.13. Water Vapor Permeability (WVP). The WVP of a film sample was determined gravimetrically through the wet cup method by Systester water vapor transmission rate tester (WVTR model–C1; SYSTESTER Instruments Co., Ltd., China), according to ASTM E96-95 standard [27]. The wet cup parameters are 38°C and 90% RH and the test area is 28.26 cm^2.

$$\mathrm{WVP} = \frac{(\mathrm{WVTR} \times L)}{\Delta p}. \tag{9}$$

The films' water vapor permeability (g/m^2 s Pa) was then calculated using formula (9), where WVTR is the measured water vapor transmission rate (g/m^2.s), L is the mean film thickness (mm), and Δp is the partial water vapor pressure difference (Pa) between both the films' two sides.

2.14. Statistical Analysis. The variance of test findings is provided in numbers. Origin 9.0 (OriginLab Co., USA) and Excel 2013 were used for graph rendering and data analysis (Microsoft Co., USA). The data were analyzed using SPSS software (version 18.0, SPSS Inc., Chicago, USA). The results were analyzed using one-way ANOVA, and then, Duncan's multiple range test was used to detect significant variations at $p < 0.05$.

3. Results and Discussion

3.1. Fourier Transform Infrared (FTIR) Spectrometry. The FTIR transmittance spectra presented in Figure 2 were used to determine the functional group and identify hydrogen bonding among PUL/CMC. The prominent peak at 3726 cm^{-1} can be ascribed to the stretching of hydroxyl groups on blend films, which is widely observed in polysaccharide polymers [17]. The stretching vibration of the (C=O) carboxyl group occurred between 1550 and 1750 cm^{-1}. The protruding peak at 2885 cm^{-1} in the samples is assigned to C-H vibration of methyl groups combined with CH_2 and CH_3 [3, 28]. Blend film samples showed peaks around 1157 and 1396 cm^{-1}, which are ascribed to antisymmetric and symmetric COO- vibrations [29]. The 1157 cm^{-1} might have been formed as a result of glycosidic bonding in polysaccharides [30]. This corresponds to the glycosidic connections' antisymmetric (1→4) expanding mode; approximately sturdy peaks at 942 cm^{-1} correspond to C-O-C stretching of α-(1-4) glycosidic links [31–33]. Furthermore, the wavenumber of this band for pullulan shifted from 1157 to 1396 cm^{-1} after blending with CMC indicating that other vibration modes may be at the recital. The wavenumber 1157 cm^{-1} is related to exocyclic C–O stretching vibrations as reported by Tong et al. [22]. It is implicit that this band may be caused by the C–OH group at the C6 position. Another band that is unique to pullulan is located at 1080 cm^{-1}. It is observed that this band is much stronger in pullulan than dextran and speculated that it is due to C–OH stretching at the C6 position for pullulan, based on the fact that all C6 atoms for dextran participated in the formation of the glycosidic C6–O–C1 linkages [34]. It is noteworthy that the wavenumber for the pullulan band remained at 1080 cm^{-1} after blending with CMC, indicating that the added polymer did not affect the vibration behavior of the C–OH group.

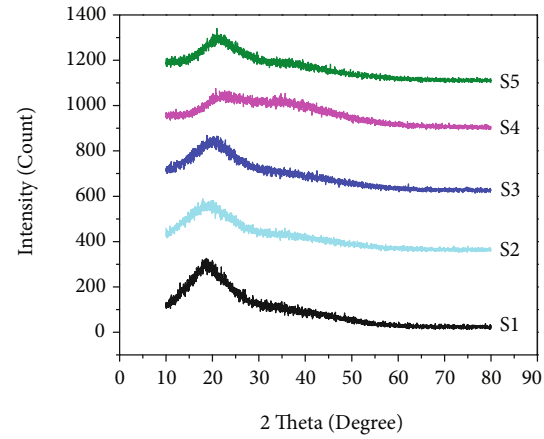

Figure 3: X-ray diffraction patterns of PUL-CMC blend films (S1-100/0, S2-75/25, S3-50/50, S4-25/75, and S5-0/100).

3.2. X-Ray Diffraction Analysis (XRD). The X-ray diffraction patterns of blend films are shown in Figure 3. The PUL film had a single broad peak at $2\theta = 19°$, denoting an amorphous structure due to the tightly-packed PUL substances with a compact hydroxyl group [3]. The observed findings reveal that by increasing the CMC concentration on the produced film, the peak intensity weakens, suggesting a decrease in crystallinity. The capacity to establish hydrogen bonds is thought to be the cause of the decrease in PUL's crystallinity. In addition, a reduction in the strength of this peak in films

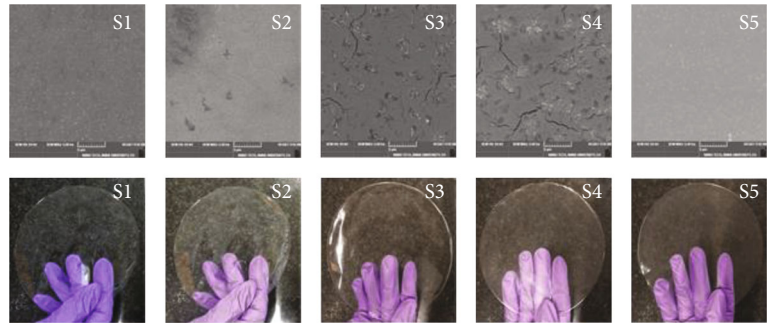

Figure 4: Scanning electron microscopy images of the samples (S1-100/0, S2-75/25, S3-50/50, S4-25/75, and S5-0/100).

with varying CMC% concentrations showed CMC was spread evenly throughout the film matrix. Due to the presence of both crystalline and amorphous provinces, the two polysaccharides used in this research are usually semicrystalline materials.

3.3. Scanning Electron Microscopy (SEM). The surface morphology of these films was investigated using SEM, as given in Figure 4. The produced films showed extreme smoothness, homogeneity with no bubbles or pores, and compact surface, thereby implying high miscibility. It may be linked to the tight arranging of PUL components with a similar characterization reported by Han et al. [17]. Increased CMC content resulted in the appearance of visible textures on the blend films' surface [19]. In comparison to pure PUL films, the blend films exhibited distinct crisscrossed patterns, representing the presence of significant interactions between PUL and CMC. Figure 4 shows that the blend films with a greater or equal percentage of PUL and CMC content S2-75/25 and S3-50/50 had a more ordered structure, whereas the films with higher CMC content S4-25/75 showed more cross-linked patterns and surface fractures. These fractures may have developed owing to the water loss and shrinkage of the surface layer during the drying process in a hot air oven and the presence of samples in a vacuum environment during SEM examination as reported by Narayanan and Lee [35]. The varied surface morphologies of blend films that are correlated to the presence of diverse hydroxyl groups and varying degrees of glycation result in the restriction of PUL and CMC molecule mobility. As shown in the XRD curves, the films with distinct amorphous nature exhibited a comparable textural difference in blend samples.

3.4. Thermogravimetric Analysis (TGA). TGA is a method that employs heat to disintegrate a substance, breaking down the connections between molecules. It is a critical approach for determining the thermal stability of materials. Figure 5(a) depicts the TGA graphs of PUL film and blended with CMC, demonstrating two main weight reduction phases. The initial weight loss stage for the pure PUL film can be ascribed to moisture vaporization at around 100°C, whereas the second weight loss step at 270°C–450°C is attributed to glycerol condensation and PUL thermal degradation, similar to the results reported by Haghighatpanah et al. [3]. TGA thermograms of blend films revealed two weight loss phases. As shown in Figure 5(a), weight loss due to evaporation occurred between 60°C and 200°C, while glycerol, PUL, and CMC breakdown occurred between 200°C and 330°C when the samples' weight was reduced to 25% and similar observations were made by Han et al. [17]. The interaction between PUL and CMC affected the TGA curves, which might be attributed to intermolecular hydrogen bonding. A broad peak at around 325°C and 300°C can be seen in Figure 5(b), which depicts the derivative thermogravimetric (DTG) curves of PUL film and blend films. The intensity of films with more PUL-S2 and S3 increased compared to films with more CMC-S4 and S5, which is associated with glycosylation breakdown and lower hydrogen bond content. The blend films deteriorated at a lower temperature and slower pace than PUL films, which might be attributed to a decrease in tightly packed PUL molecules.

3.5. Thickness, Density, and Mechanical Properties of the Film. The effects of various percentages of PUL and CMC concentrations on the thickness, density, and mechanical characteristics of blend films are shown in Table 1. From 0.16 mm to 0.12 mm, the thickness of PUL/CMC films did not vary much. Although the impact of loading PUL on density was not significant ($p > 5\%$), the density of the films was greater than that of the CMC film, suggesting that S2 and S3 films were more compact. These findings are in line with those reported by Han et al. [17]. PUL may have reacted with CMC in the film matrix, initiating interactions including hydrogen bonds, according to FTIR findings of Tong et al. [22]. For a packaging film to resist external stress and retain its integrity as well as barrier characteristics throughout uses in packing, it must have sufficient mechanical strength and extensibility. To enhance mechanical characteristics, polysaccharide blends with various polymer percentages may be helpful. The films' tensile strength (TS) and percentage of elongation (EAB%) were measured, and the results are shown in Table 1. An equivalent percentage or more than 50% of PUL blended with CMC films results in tensile strength ranging from 17.30 MPa to 9.28 MPa. The obtained results of tensile strength of the produced film are compared with the commercially available polylactic acid (PLA) cross-linked film [36]. The development of hydrogen bond between the -OH of the PUL may explain the high TS values. The current study's TS values were greater than those

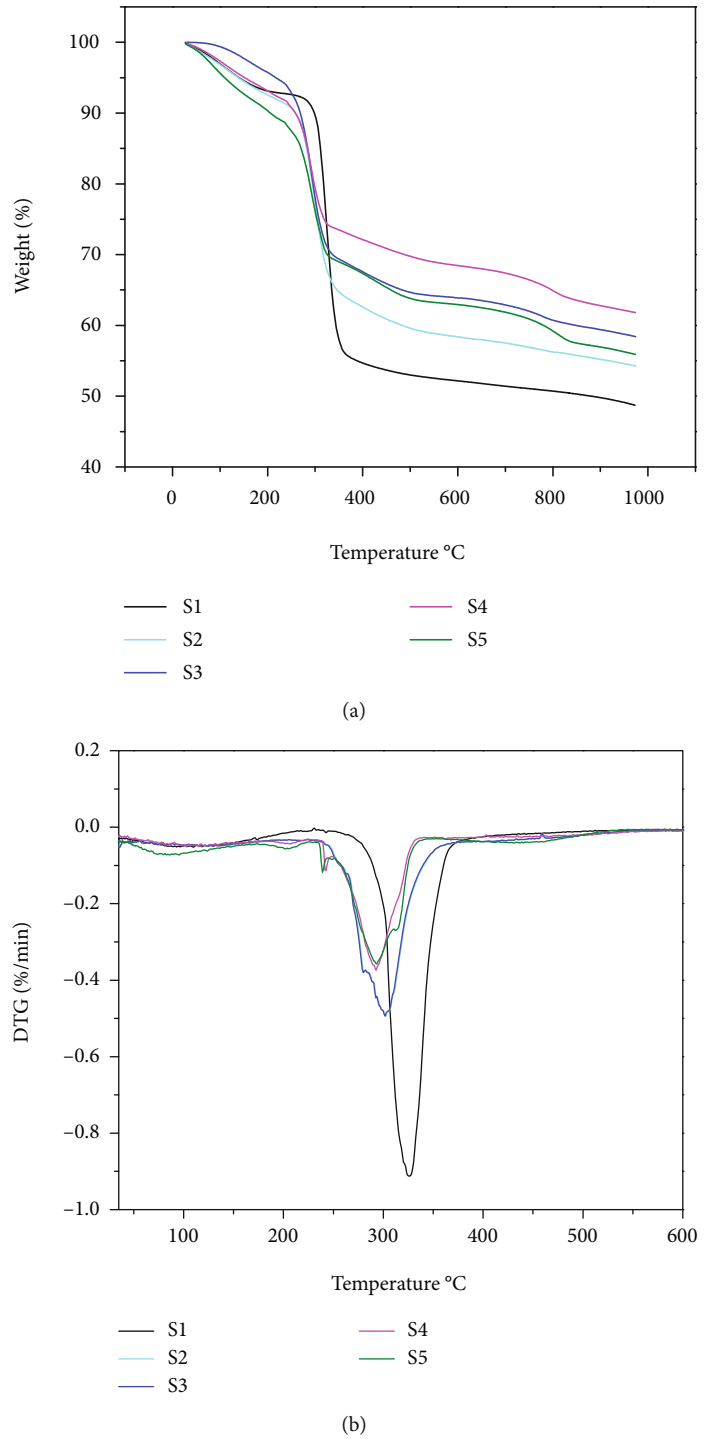

Figure 5: (a) Weight loss. (b) DTG. Film samples (S1-100/0, S2-75/25, S3-50/50, S4-25/75, and S5-0/100).

published in the literature, which might be related to the CH composition, presence of plasticizer, and film production technique [37]. However, when the concentration of CMC increased in the blends, the tensile strength of the films dropped substantially. This study's film may be utilized inside the packaging of certain pharmaceutical products. In general, the TS requirements for this kind of edible film were quite modest.

3.6. Colour Parameter. The colour of packaging films has a great effect on the aesthetic, consumer acceptance, and food and pharmaceutical products' package quality. Colour functions such as ΔE indicate the degree of total colour difference from the standard colour plate, YI indicates the degree of yellowness, and WI indicates the degree of whiteness, which may be due to the increasing concentration in CMC on PUL Table 2. While YI and WI decreased significantly ($p < 0.05$)

Table 1: Mechanical properties of the blend films.

Sample	Thickness (mm)	Density (g/mm^2)	TS (MPa)	EAB (%)
S1	0.121 ± 0.011^{a}	0.146 ± 0.019^{b}	30.53 ± 0.850^{d}	04.09 ± 0.263^{a}
S2	0.164 ± 0.011^{b}	0.094 ± 0.015^{a}	17.30 ± 0.954^{c}	05.55 ± 1.210^{a}
S3	0.167 ± 0.036^{b}	0.094 ± 0.017^{a}	08.60 ± 0.524^{a}	31.42 ± 1.000^{b}
S4	0.125 ± 0.013^{a}	0.147 ± 0.031^{b}	09.28 ± 0.223^{a}	48.37 ± 1.150^{c}
S5	0.136 ± 0.009^{ab}	0.109 ± 0.005^{a}	12.40 ± 1.735^{b}	54.47 ± 1.607^{d}

Different superscript letters (a–d) indicate significant differences among formulations ($p < 0.05$).

Table 2: Colour parameters of the blend films.

Sample	L^*	a^*	b^*	ΔE	BI	WI	YI
S1	36.234 ± 0.027^{e}	0.551 ± 0.013^{d}	0.061 ± 0.017^{a}	—	9.100 ± 0.010^{e}	8.779 ± 0.012^{d}	1.456 ± 0.288^{a}
S2	35.946 ± 0.162^{d}	0.468 ± 0.020^{b}	0.712 ± 0.099^{b}	0.718 ± 0.163^{a}	8.797 ± 0.113^{d}	8.170 ± 0.171^{c}	3.751 ± 0.463^{b}
S3	35.295 ± 0.031^{c}	0.424 ± 0.013^{a}	1.179 ± 0.124^{c}	1.466 ± 0.120^{b}	8.345 ± 0.054^{c}	7.533 ± 0.103^{b}	5.658 ± 0.630^{c}
S4	35.133 ± 0.084^{b}	0.422 ± 0.014^{a}	2.003 ± 0.027^{d}	2.246 ± 0.019^{c}	8.057 ± 0.016^{b}	6.823 ± 0.013^{a}	9.035 ± 0.253^{d}
S5	34.874 ± 0.064^{a}	0.523 ± 0.015^{c}	1.963 ± 0.011^{d}	2.340 ± 0.029^{c}	7.934 ± 0.032^{a}	6.658 ± 0.035^{a}	8.734 ± 0.541^{d}

Different superscript letters (a–d) indicate significant differences among formulations ($p < 0.05$).

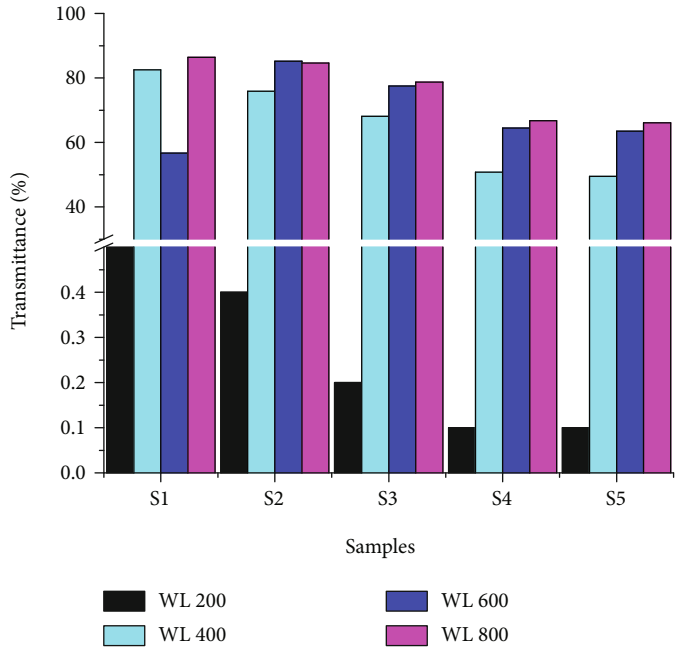

Figure 6: Light transmittance for blended film (S1-100/0, S2-75/25, S3-50/50, S4-25/75, and S5-0/100).

as a result of increased CMC concentration, ΔE increased considerably. The components of two polysaccharide integrated films significantly reduced the value of $L*$ and the brightness. However, as the quantity of CMC increased, the value of $a*$ decreased considerably, while $b*$ greatly increased. The blend films became darker, redder, and yellower compared with the pure PUL and CMC films, after adding CMC. In addition, the ΔE value of blend films with above 50 percent CMC addition was very high compared with other blend films. Hence, the blend films became slightly greenish and yellowish, but they were still transparent. Furthermore, a visual observation confirmed this fact.

3.7. Light Transmittance Properties. Light transparency is a critical property for packaging films, which affects their general appearance and determines their packaging applications. Light transmission in the UV and visible light range at selected wavelengths is from 200 nm to 800 nm, and the transparency of the films is shown in Figure 6. The transmission of UV light is found to be very low at 200 nm when there is an increase of CMC with pullulan films, similar to the results reported by Mu et al. [38]. This results in a relatively UV barrier capacity at 200 nm wavelength for the gelatin films in comparison with other commercially available PLA and starch films [39]. As a result, blend films have

Table 3: Moisture properties of the blend films.

Sample	WVP ($\times 10^{-10}$ g m^{-1}s^{-1}Pa^{-1})	Moisture content (%)	Contact angle
S1	2.60	17.21 ± 0.58^{c}	66.70 ± 2.87^{a}
S2	4.12	20.77 ± 0.44^{bc}	63.43 ± 2.84^{b}
S3	5.75	22.20 ± 1.25^{ab}	54.82 ± 1.20^{b}
S4	4.99	26.19 ± 1.15^{a}	58.90 ± 2.75^{c}
S5	5.34	30.35 ± 0.95^{a}	55.55 ± 2.61^{d}

Different superscript letters (a–d) indicate significant differences among formulations ($p < 0.05$).

excellent barrier properties against UV light in the region, which induces lipid oxidation in any edible substance. These properties shield the PUL/CMC blend films from light, enabling them to provide increased protection to packaged medicine in capsules against discolouration, off-flavor, and nutrient losses caused by light-induced oxidation. Therefore, it contributes to preserving the quality of packaged drugs and food products and increases their shelf-life.

3.8. Moisture Content (MC). Traditionally, the moisture content, contact angle, and water vapor permeability of packaging films were conducted to estimate their water resistance. Generally, the lower the moisture content and WVP, and the greater the contact angle, the better the films' water protection. The MC of pure PUL film was the lowest (17.20%), while S4 film had the greatest MC (26.18%). The addition of CMC raised the MC content of blend films from 20.76% to 26.18%. In general, the inclusion of CMC enhanced the MC of films based on polysaccharides [38]. The scientific explanation is that CMC appears to contain several hydroxyl groups, which significantly raise the hydrophilicity of the film, resulting in a higher MC [16]. The addition of 30% (*w*/*v*) glycerol resulted in a significant increase in WVP values and moisture content for all tested films. This could be owing to the increased hydrophilicity of the film following the addition of polyol and the increased plasticity of the polymer chain due to the plasticizing effect of glycerol, which increases the dispersibility of water molecules in the blend films.

3.9. Contact Angle. The contact angle of a film provides information about its surface hydrophilicity. The addition of CMC in pullulan-based films caused a decrease in the water contact angle value (from 63° to 59°), as shown in Table 3. The surface hydrophilicity of the films was marginally increased with the addition of CMC, while the contact angle of the integrated film was stabilized in the S2 sample at 63°. This implicates that the hydrophilicity of the CMC loaded with PUL is connected to the surface structure and moisture content. Higher contact angles are usually associated with a change in surface hydrophobicity and surface roughness, as reported by Crouvisier-Urion et al. [40]. The surface roughness of films containing S2 is greater in this scenario, and this is shown to be closely connected to the homogenization process during film-making [41]. In this context, the ability to design and influence the hydrophilic-hydrophobic character of hybrid systems with many outstanding properties appears to be the key to developing compatible biomaterials that are edible and effective in drug delivery systems [42].

3.10. Water Vapor Permeability. The WVP data for pure PUL, CMC, and blend films are summarized in Table 3. PUL film had lower WVP 2.60×10^{-10} g m^{-1}s^{-1}Pa^{-1} compared to CMC 5.34×10^{-10} g m^{-1}s^{-1}Pa^{-1} films. The polysaccharide films form weak barriers to water vapor as they are relatively hydrophilic [43]. The WVP of the produced blend films increased as a result of the incorporation of CMC on PUL, most likely due to the increased free volume of the polymer blend produced by CMC's bulkier anionic side group. The addition of 30% (*w*/*v*) of glycerol resulted in a dramatic increase in WVP values for all films tested. This can be attributed to the increased film hydrophilicity caused by the added glycerol and the enhanced polymer chain mobility due to the plasticization effect of glycerol, which increased the diffusivity of water molecules in the film matrix. This agreed with the tensile data, which showed that (PUL/CMC) 75/25 percentage is the strongest (highest TS and moderate EAB%) among the prepared blend films.

4. Conclusion

In conclusion, blends of PUL and CMC are of special importance in the field of the pharmaceutical industry as an alternative material for cellulose and gelatin. The original structure of pullulan and CMC was remodeled, which attributed to the new hydrogen bonds. CMC-added films were more flexible than pure pullulan film and the toughest one, while the pullulan and CMC with the percentage of 75/25 film showed the best water barrier and mechanical properties. Meanwhile, the thermal decomposition of the S2 blend film transpired more slowly. The surface of all the produced films was the transparent and light barrier, and SEM analysis confirmed S2 blend film with smooth and clear miscibility. Therefore, pullulan and CMC blended film is a potential candidate for preparing the edible film. This research provides a better understanding of how PUL interacts with CMC and the rationale for the design of edible blend films for pharmaceutical packaging applications, which is an alternative material (gelatin and cellulose) for capsule production.

Data Availability

The data used to support the findings of this study are included within the article.

Conflicts of Interest

The authors declare that there is no conflict of interest regarding the publication of this paper.

Acknowledgments

The authors wish to express their gratefulness to the Department of Printing Technology, Anna University, Chennai,

600025, and Prof. CNR Rao Research Centre, Coimbatore, 641043, Tamil Nadu, India, for supporting the facilities for this research work and technical assistance.

References

[1] S. Farris, I. U. Unalan, L. Introzzi, J. Fuentes-Alventosa, and C. Cozzolino, "Pullulan-based films and coatings for food packaging: present applications, emerging opportunities, and future challenges," *Journal of Applied Polymer Science*, vol. 131, no. 13, pp. 1–12, 2014.

[2] L. Liu, M. Yang, J. Xu et al., "Exploring the role of pullulan in the process of potato starch film formation," *Carbohydrate Polymers*, vol. 234, p. 115910, 2020.

[3] N. Haghighatpanah, M. Omar-Aziz, M. Gharaghani, F. Khodaiyan, S. Hosseini, and J. Kennedy, "Effect of mung bean protein isolate/pullulan films containing marjoram (*Origanum majorana* L.) essential oil on chemical and microbial properties of minced beef meat," *International Journal of Biological Macromolecules*, vol. 201, pp. 318–329, 2022.

[4] E. A. Arik Kibar and F. Us, "Thermal, mechanical and water adsorption properties of corn starch- carboxymethylcellulose/methylcellulose biodegradable films," *Journal of Food Engineering*, vol. 114, no. 1, pp. 123–131, 2013.

[5] P. Kanmani and S. T. Lim, "Development and characterization of novel probiotic-residing pullulan/starch edible films," *Food Chemistry*, vol. 141, no. 2, pp. 1041–1049, 2013.

[6] X. Jia, Z. Qin, J. Xu, B. Kong, Q. Liu, and H. Wang, "Preparation and characterization of pea protein isolate-pullulan blend electrospun nanofiber films," *International Journal of Biological Macromolecules*, vol. 157, pp. 641–647, 2020.

[7] B. Saberi, R. Thakur, Q. V. Vuong et al., "Optimization of physical and optical properties of biodegradable edible films based on pea starch and guar gum," *Industrial Crops and Products*, vol. 86, pp. 342–352, 2016.

[8] J. Sadeghizadeh-Yazdi, M. Habibi, A. A. Kamali, and M. Banaei, "Application of edible and biodegradable starch-based films in food packaging: a systematic review and meta-analysis," *Current Research in Nutrition and Food Science*, vol. 7, no. 3, pp. 624–637, 2019.

[9] D. Wei, H. Wang, H. Xiao, A. Zheng, and Y. Yang, "Morphology and mechanical properties of poly(butylene adipate-co- terephthalate)/potato starch blends in the presence of synthesized reactive compatibilizer or modified poly(butylene adipate-co-terephthalate)," *Carbohydrate Polymers*, vol. 123, pp. 275–282, 2015.

[10] R. Bhat, N. Abdullah, R. H. Din, and G. S. Tay, "Producing novel sago starch based food packaging films by incorporating lignin isolated from oil palm black liquor waste," *Journal of Food Engineering*, vol. 119, no. 4, pp. 707–713, 2013.

[11] T. J. Gutierrez, M. S. Tapia, E. Perez, and L. Fama, "Structural and mechanical properties of edible films made from native and modified cush-cush yam and cassava starch," *Food Hydrocolloids*, vol. 45, pp. 211–217, 2015.

[12] L. Sheng, P. Li, H. Wu et al., "Tapioca starch-pullulan interaction during gelation and retrogradation," *Lwt*, vol. 96, pp. 432–438, 2018.

[13] H. Mirzaee, F. Khodaiyan, J. F. Kennedy, and S. S. Hosseini, "Production, optimization and characterization of pullulan from sesame seed oil cake as a new substrate by *Aureobasidium pullulans*," *Carbohydrate Polymer Technologies and Applications*, vol. 1, p. 100004, 2020.

[14] P. Shao, B. Niu, H. Chen, and P. Sun, "Fabrication and characterization of tea polyphenols loaded pullulan-CMC electrospun nanofiber for fruit preservation," *International Journal of Biological Macromolecules*, vol. 107, pp. 1908–1914, 2018.

[15] G. Chen, Y. Zhu, G. Zhang et al., "Optimization and characterization of pullulan production by a newly isolated high-yielding strain Aureobasidium melanogenum," *Preparative Biochemistry and Biotechnology*, vol. 49, no. 6, pp. 557–566, 2019.

[16] G. Zhu, L. Sheng, and Q. Tong, "Preparation and characterization of carboxymethyl-gellan and pullulan blend films," *Food Hydrocolloids*, vol. 35, pp. 341–347, 2014.

[17] K. Han, Y. Liu, Y. Liu, X. Huang, and L. Sheng, "Characterization and film-forming mechanism of egg white/pullulan blend film," *Food Chemistry*, vol. 315, p. 126201, 2020.

[18] D. Kowalczyk, M. Kordowska-Wiater, M. Karas, E. Zieba, M. Monika, and A. E. Wiacek, "Release kinetics and antimicrobial properties of the potassium sorbate-loaded edible films made from pullulan, gelatin and their blends," *Food Hydrocolloids*, vol. 101, p. 105539, 2020.

[19] W. Lan, R. Zhang, T. Ji et al., "Improving nisin production by encapsulated *Lactococcus lactis* with starch/carboxymethyl cellulose edible films," *Carbohydrate Polymers*, vol. 251, p. 117062, 2021.

[20] J. Wu, F. Zhong, Y. Li, C. F. Shoemaker, and W. Xia, "Preparation and characterization of pullulan-chitosan and pullulan-carboxymethyl chitosan blended films," *Food Hydrocolloids*, vol. 30, no. 1, pp. 82–91, 2013.

[21] M. Omar-Aziz, F. Khodaiyan, M. S. Yarmand et al., "Combined effects of octenylsuccination and beeswax on pullulan films: water- resistant and mechanical properties," *Carbohydrate Polymers*, vol. 255, p. 117471, 2021.

[22] Q. Tong, Q. Xiao, and L. T. Lim, "Preparation and properties of pullulan-alginate-carboxymethylcellulose blend films," *Food Research International*, vol. 41, no. 10, pp. 1007–1014, 2008.

[23] K. Lupina, D. Kowalczyk, E. Zieba et al., "Edible films made from blends of gelatin and polysaccharide-based emulsifiers - a comparative study," *Food Hydrocolloids*, vol. 96, pp. 555–567, 2019.

[24] C. Ruan, Y. Zhang, J. Wang et al., "Preparation and antioxidant activity of sodium alginate and carboxymethyl cellulose edible films with epigallocatechin gallate," *International Journal of Biological Macromolecules*, vol. 134, pp. 1038–1044, 2019.

[25] ASTM, *Standard Test Method for Tensile Properties of Thin Plastic Sheeting*, Standard D882, American Society for Testing and Materials, Philadelphia, PA, USA, 2001.

[26] F. S. Mostafavi, R. Kadkhodaee, B. Emadzadeh, and A. Koocheki, "Preparation and characterization of tragacanth-locust bean gum edible blend films," *Carbohydrate Polymers*, vol. 139, pp. 20–27, 2016.

[27] L. F. Wang, J. W. Rhim, and S. I. Hong, "Preparation of poly(lactide)/poly(butylene adipate-co-terephthalate) blend films using a solvent casting method and their food packaging application," *LWT - Food Science and Technology*, vol. 68, pp. 454–461, 2016.

[28] M. Hamidi, J. F. Kennedy, F. Khodaiyan, Z. Mousavi, and S. S. Hosseini, "Production optimization, characterization and gene

expression of pullulan from a new strain of *Aureobasidium pullulans*," *International Journal of Biological Macromolecules*, vol. 138, pp. 725–735, 2019.

[29] C. Xiao, L. Weng, and L. Zhang, "Improvement of physical properties of crosslinked alginate and carboxymethyl konjac glucomannan blend films," *Journal of Applied Polymer Science*, vol. 84, no. 13, pp. 2554–2560, 2002.

[30] M. Kacurakova, P. Capek, V. Sasinkova, N. Wellner, and A. Ebringerova, "FT-IR study of plant cell wall model compounds: pectic polysaccharides and hemicelluloses," *Carbohydrate Polymers*, vol. 43, no. 2, pp. 195–203, 2000.

[31] M. Bercea, G. Biliuta, M. Avadanei, R. I. Baron, M. Butnaru, and S. Coseri, "Self-healing hydrogels of oxidized pullulan and poly(vinyl alcohol)," *Carbohydrate Polymers*, vol. 206, pp. 210–219, 2019.

[32] B. Niu, P. Shao, H. Chen, and P. Sun, "Structural and physiochemical characterization of novel hydrophobic packaging films based on pullulan derivatives for fruits preservation," *Carbohydrate Polymers*, vol. 208, pp. 276–284, 2019.

[33] M. Michelin, A. M. Marques, L. M. Pastrana, J. A. Teixeira, and M. A. Cerqueira, "Carboxymethyl cellulose-based films: effect of organosolv lignin incorporation on physicochemical and antioxidant properties," *Journal of Food Engineering*, vol. 285, p. 110107, 2020.

[34] K. I. Shigel, "Determination of structural peculiarities of dexran, pullulan and γ-irradiated pullulan by Fourier-transform IR spectroscopy," *Carbohydrate Research*, vol. 337, no. 16, pp. 1445–1451, 2002.

[35] T. S. N. S. Narayanan and M. H. Lee, "A simple strategy to modify the porous structure of plasma electrolytic oxidation coatings on magnesium," *RSC Advances*, vol. 6, no. 19, pp. 16100–16114, 2016.

[36] S. Sharma, A. K. Jaiswal, B. Duffy, and S. Jaiswal, "Ferulic acid incorporated active films based on poly(lactide) /poly(butylene adipate-co-terephthalate) blend for food packaging," *Food Packaging and Shelf Life*, vol. 24, p. 100491, 2020.

[37] M. S. Rao, S. R. Kanatt, S. P. Chawla, and A. Sharma, "Chitosan and guar gum composite films: preparation, physical, mechanical and antimicrobial properties," *Carbohydrate Polymers*, vol. 82, no. 4, pp. 1243–1247, 2010.

[38] C. Mu, J. Guo, X. Li, W. Lin, and D. Li, "Preparation and properties of dialdehyde carboxymethyl cellulose crosslinked gelatin edible films," *Food Hydrocolloids*, vol. 27, no. 1, pp. 22–29, 2012.

[39] S. Saez-Orviz, I. Marcet, S. Weng, M. Rendueles, and M. Diaz, "PLA nanoparticles loaded with thymol to improve its incorporation into gelatine films," *Journal of Food Engineering*, vol. 269, p. 109451, 2020.

[40] K. Crouvisier-Urion, A. Lagorce-Tachon, C. Lauquin et al., "Impact of the homogenization process on the structure and antioxidant properties of chitosan-lignin composite films," *Food Chemistry*, vol. 236, pp. 120–126, 2017.

[41] A. E. Wiacek and K. Dul, "Effect of surface modification on starch/phospholipid wettability," *Colloids and Surfaces A: Physicochemical and Engineering Aspects*, vol. 480, pp. 351–359, 2015.

[42] K. Przykaza, M. Jurak, A. E. Wiącek, and R. Mroczka, "Characteristics of hybrid chitosan/phospholipid-sterol, peptide coatings on plasma activated PEEK polymer," *Materials Science and Engineering C*, vol. 120, p. 111658, 2021.

[43] M. M. Marvizadeh, Z. Oladzadabbasabadi, A. Mohammadi Nafchi, and M. Jokar, "Preparation and characterization of bionanocomposite film based on tapioca starch/bovine gelatin/nanorod zinc oxide," *International Journal of Biological Macromolecules*, vol. 99, pp. 1–7, 2017.